

Experimental test of models of radio-frequency plasma sheaths

M. A. Sobolewski^{a)}

National Institute of Standards and Technology, Gaithersburg, Maryland 20899

(Received 14 November 1996; accepted for publication 11 December 1996)

The ion current and sheath impedance were measured at the radio-frequency-powered electrode of an asymmetric, capacitively coupled plasma reactor, for discharges in argon at 1.33–133 Pa. The measurements were used to test the models of the radio frequency sheath derived by Lieberman [IEEE Trans. Plasma Sci. **17**, 338 (1989)] and Godyak and Sternberg [Phys. Rev. A **42**, 2299 (1990)], and establish the range of pressure and sheath voltage in which they are valid. © 1997 American Institute of Physics. [S0003-6951(97)01008-5]

Radio-frequency (rf) discharges are widely used in the semiconductor industry. The electrical properties of these discharges are usually dominated by the rf sheaths that separate rf electrodes from the plasma. Models^{1–3} have been proposed to predict the electrical properties of rf sheaths and relate them to the dynamics of particles within the sheaths. In the high frequency range, where the sheath is primarily capacitive, Lieberman has derived analytic models for a low pressure, collisionless sheath¹ and a higher pressure, highly collisional sheath.² Godyak and Sternberg have developed a model³ to cover the entire pressure range and have solved it numerically. These models are used to explain electrical data,⁴ to investigate the electrical interaction between the plasma and its surroundings,⁵ and to reduce the computational requirements of computer simulations of discharge.⁶ Some of these results may be in doubt, however, because sheath models have not been sufficiently tested by experiment. One experimental test of sheath models has been reported³ in a symmetric discharge, for mercury vapor at a pressure of 0.16 Pa, in the collisionless range. Tests at higher pressures and in asymmetric discharges have not been reported; they are the subject of this work.

In the high-pressure, collisional Lieberman model,² the capacitive impedance of the sheath, Z_c , can be expressed as

$$Z_c = 0.803 \left(\frac{e}{\omega^5 \epsilon_0^3 A^3 m_i} \right)^{1/5} V_c^{3/5} I_0^{-2/5} \lambda_i^{1/5}, \quad (1)$$

where e is the charge of an electron, ω is the fundamental rf frequency, ϵ_0 is the permittivity of vacuum, A is the electrode area, m_i is the ion mass, λ_i is the ion diffusivity mean free path, V_c is the amplitude of the fundamental component of the sheath voltage, and I_0 is the dc ion current,

$$I_0 = en_0 u_0 A. \quad (2)$$

Here, n_0 and u_0 are the ion density and velocity at the plasma/sheath boundary. The predictions of sheath models are often expressed in terms of n_0 , but I_0 is a better experimental parameter. It is difficult to measure n_0 . Because of gradients in ion density, values of the ion density measured in the bulk plasma may differ from n_0 . The gradient of ion current, however, is smaller. Indeed, it is zero for any region where no ionization or recombination occurs, a valid assumption for most if not all of the sheath region. Furthermore, using I_0 in Eq. (1) eliminates the u_0 dependence, so no

assumption need be made regarding u_0 . Although, in Refs. 1 and 2, u_0 was assumed to be the Bohm velocity, Eq. (1) is valid for any value of u_0 .

Here, we test Eq. (1) for the sheath at the powered electrode of a capacitively coupled, parallel-plate reactor (Fig. 1) for discharges in argon at 1.33–133 Pa. Previously, mass spectrometry⁷ has determined that the dominant ion in these discharges is Ar^+ . Ar^+ ions, accelerated in the sheath to energies of 1–100 eV, lose momentum primarily through charge exchange collisions with argon neutrals. Therefore, λ_i , which describes the rate of loss of ion momentum due to collisions, can be determined from measured values⁸ of Q_{ct} , the cross section of Ar^+/Ar charge exchange collisions. A value of $Q_{ct} = 4.3 \times 10^{-15} \text{ cm}^2$, measured for ions at an intermediate energy (12 eV), was used, and λ_i was obtained from $\lambda_i = (N Q_{ct})^{-1}$, where N is the number density of the neutral gas at the measured pressure, at standard temperature. The electrode area A was 81.1 cm^2 and $\omega/2\pi$ was 13.56 MHz.

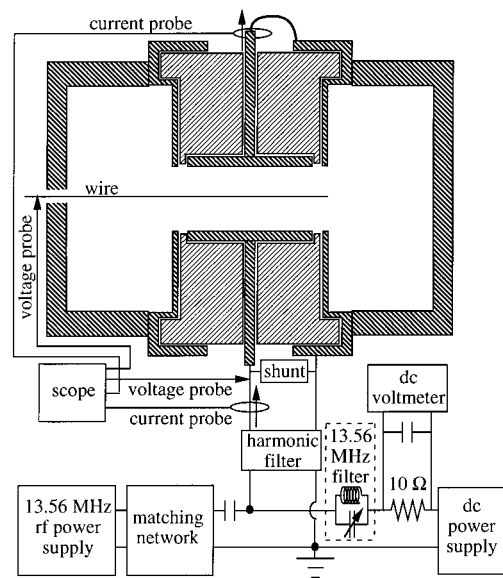


FIG. 1. Diagram of the discharge cell (described in detail in Ref. 4) and the experimental apparatus. The upper electrode and the walls of the vacuum chamber are grounded, while the lower electrode was driven simultaneously by a 13.56 MHz power supply (coupled through a matching network and blocking capacitor) and a dc power supply. To prevent the dc power supply from short circuiting the rf power supply and the plasma, a tuned 13.56 MHz filter was inserted on the dc power lead. The dc current supplied to the electrode was determined from the voltage across a 10 Ω resistor.

^{a)}Electronic mail: sobo@enh.nist.gov

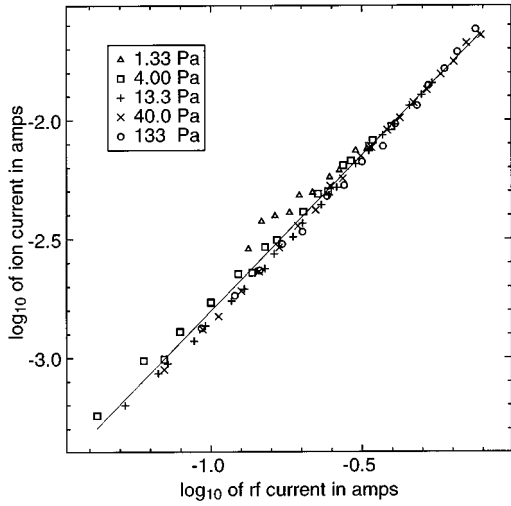


FIG. 2. Log–log plot of I_0 , the ion current at the powered electrode, vs I_{pe} , the fundamental (13.56 MHz) component of the rf current at the powered electrode, for argon discharges at pressures of 1.33–133 Pa. A linear fit to the data, corresponding to a power-law dependence of I_0 on I_{pe} is also shown.

The ion current, I_0 , was measured by a method⁹ in which the rf-powered electrode is simultaneously driven by a dc power supply to a large, negative dc voltage that repels plasma electrons from the electrode, allowing collection and measurement of a dc current that consists solely of ions. Because the application of the dc bias perturbs the plasma, the measured ion current is not constant at large negative bias. To obtain the unperturbed value of the ion current, an extrapolation procedure,⁹ linear with dc voltage, was used. The ion currents obtained by this procedure, plotted in Fig. 2, display a power-law dependence on the rf current, and are nearly independent of pressure.

As described previously,⁴ the sheath impedance, Z_{ps} , was determined from measurements of the rf current and voltage on the powered electrode and the rf voltage on a wire probe inserted into the plasma. In addition to the sheath capacitance, Z_{ps} includes series and parallel resistances. Procedures^{4,10,11} that fit $\text{Re}(Z_{ps})$ data were used to determine these resistances, the capacitive impedance Z_c , and the voltage across it, V_c . Figure 3 shows a log–log plot of Z_c versus V_c . At pressures ≥ 4.0 Pa and voltages ≥ 100 V, Z_c follows a power-law dependence on pressure and voltage. Below 4 Pa, Z_c becomes less sensitive to pressure. This indicates the beginning of the transition from the collisional regime of Ref. 2 to the collisionless regime of Ref. 1.

To compare the data to the Lieberman collisional model, Eq. (1), experimental values of Z_c from 4 to 133 Pa were multiplied by $I_0^{2/5} \lambda_i^{-1/5}$ and plotted versus V_c on a log–log scale in Fig. 4. On this plot, the prediction of the Lieberman model, Eq. (1), is a straight line of slope 0.60, as shown. At $V_c \geq 100$ V, the experimental points also fall close to a single straight line with the same slope, indicating that, in this range, the $V_c^{3/5} I_0^{-2/5} \lambda_i^{1/5}$ dependence predicted by Eq. (1) is consistent with the data. Nevertheless, the experimental data are always higher than the Lieberman model.

Also shown in Fig. 4 are predictions from the Godyak–Sternberg model,³ calculated for an electron temperature

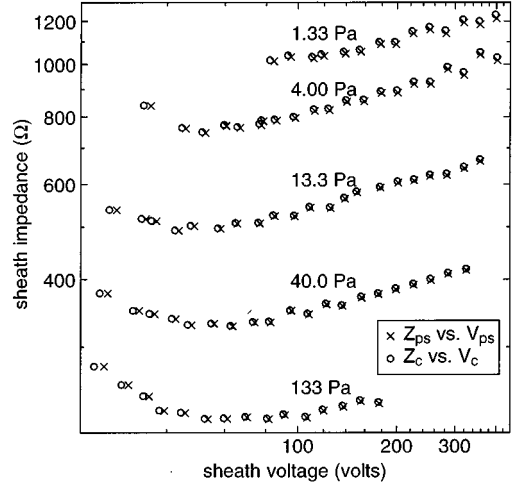


FIG. 3. Log–log plot of the fundamental (13.56 MHz) amplitudes of the voltage and impedance of the sheath at the powered electrode of argon discharges at 1.33–133 Pa. The total impedance and voltage, Z_{ps} and V_{ps} , are plotted, as well as the capacitive components Z_c and V_c .

$T_e = 3$ eV, measured afterwards, in the same cell, by a Langmuir probe, for argon discharges at 4–40 Pa. This value of T_e yields Maxwellian distributions that are fair overall fits to the non-Maxwellian electron energy distribution functions measured at 4–133 Pa in a nearly identical cell.¹² (In either cell, no T_e measurements have been achieved or reported at 1.33 Pa.) The Godyak–Sternberg model also requires values for a collisional parameter,

$$\alpha = (\pi \lambda_d / 2 \lambda_i) = (\pi / 2 \lambda_i) (\epsilon_0 T_e / n_0 e)^{0.5}, \quad (3)$$

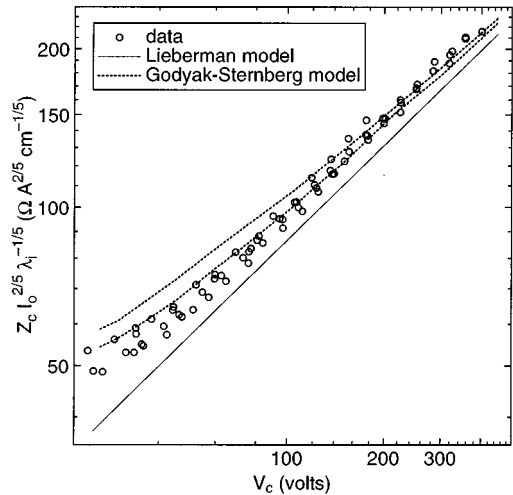


FIG. 4. Log–log plot of $Z_c I_0^{2/5} \lambda_i^{-1/5}$ vs V_c , in which the predictions of the Lieberman model, Eq. (1), fall on a single line. The plot shows experimental data for argon discharges at 4.0–133.3 Pa, the Lieberman results (solid line), and results from the model of Godyak and Sternberg. As the input parameters are varied over the range of experimental conditions, the Godyak–Sternberg results vary with α in the range defined by the two dotted curves. Results from high values of α , i.e., high pressures, define the upper dotted curve; results from low values of α , i.e., low pressures, define the lower dotted curve.

that describes the size of the mean free path, λ_i , relative to the Debye length, λ_d . The Godyak–Sternberg model assumes an ion injection velocity u_0 of

$$u_0 = \{eT_e/[m_i(1 + \alpha)]\}^{1/2}. \quad (4)$$

For $T_e = 3$ eV, values of α , n_0 , and u_0 were determined at each data point ≥ 4.0 Pa by solving Eqs. (2)–(4) iteratively at measured values of the ion current I_0 . Values of α increased with pressure and decreased with voltage, in the range $0.17 \leq \alpha \leq 8.7$. The Godyak and Sternberg predictions were then obtained by digitizing and interpolating Fig. 9 of Ref. 3, which gives numerical results for the dependence of Z_c on α , n_0 , and sheath voltage. Unlike the Lieberman model, the Godyak and Sternberg results in Fig. 4 show curvature at low voltages. The Lieberman model assumes that the minimum sheath width W_{\min} is zero; that is, once per cycle the sheath contracts to zero thickness. Therefore, as $V_c \rightarrow 0$, $Z_c \rightarrow 0$. In contrast, in the Godyak and Sternberg model, W_{\min} is nonzero, and Z_c approaches a nonzero value as $V_c \rightarrow 0$. This effect produces the curvature seen in the Godyak and Sternberg model and in the data.

Reference 9 estimates the uncertainty of the I_0 measurement technique as $\leq 30\%$. This produces an uncertainty of 13% in $Z_c I_0^{2/5} \lambda_i^{-1/5}$. Differences between the Lieberman model and the data are larger, up to 40%. This disagreement cannot be explained by plasma nonuniformity. Although simulations¹³ of these discharges at pressures ≥ 4.0 Pa do show radial variations in the ion current density and sheath voltage, the net effect of these variations changes the values of Z_c predicted by Eq. (1) by less than 1%. In the Godyak and Sternberg model, an uncertainty of ± 1 eV in T_e introduces an uncertainty in $Z_c I_0^{2/5} \lambda_i^{-1/5}$ that varies from $\pm 9\%$ at the lowest voltage, to $< 1\%$ at the highest voltage. Within

the uncertainties arising from T_e and I_0 , the Godyak and Sternberg model agrees with the data. The agreement is particularly good at sheath voltages > 100 V. Agreement was obtained despite the fact that at least one assumption of the Godyak and Sternberg model—the assumption of a sinusoidal current waveform—is not valid in the asymmetric discharges studied here.

In conclusion, the power-law dependence of sheath impedance on pressure and sheath voltage predicted by the Lieberman collisional model was observed at pressures ≥ 4.0 Pa and sheath voltages ≥ 100 V. The values of the sheath impedance predicted by the Lieberman model were not, however, in agreement with the measurements. The Godyak–Sternberg model was in agreement with the data. In addition to confirming the Godyak and Sternberg model, the agreement validates the experimental usefulness of ion current measurements in experimental tests of sheath models.

¹M. A. Lieberman, IEEE Trans. Plasma Sci. **16**, 638 (1988).

²M. A. Lieberman, IEEE Trans. Plasma Sci. **17**, 338 (1989).

³V. A. Godyak and N. Sternberg, Phys. Rev. A **42**, 2299 (1990).

⁴M. A. Sobolewski, IEEE Trans. Plasma Sci. **23**, 1006 (1995).

⁵M. Surendra, C. R. Guarnieri, G. S. Selwyn, and M. Dalvie, Appl. Phys. Lett. **66**, 2415 (1995).

⁶T. E. Nitschke and D. B. Graves, IEEE Trans. Plasma Sci. **23**, 717 (1995).

⁷J. K. Olthoff, R. J. Van Brunt, S. B. Radovanov, J. A. Rees, and R. Surowiec, J. Appl. Phys. **75**, 115 (1994).

⁸M. V. V. S. Rao, R. J. Van Brunt, and J. K. Olthoff, Phys. Rev. E **54**, 5641 (1996).

⁹V. A. Godyak, R. B. Piejak, and B. M. Alexandrovich, J. Appl. Phys. **69**, 3455 (1991).

¹⁰V. A. Godyak, R. B. Piejak, and B. M. Alexandrovich, IEEE Trans. Plasma Sci. **19**, 660 (1991).

¹¹L. J. Overzet and F. Y. Leong-Rousey, Plasma Sources Sci. Technol. **4**, 432 (1995).

¹²M. B. Hopkins, J. Res. Natl. Inst. Stand. Technol. **100**, 415 (1995).

¹³J. P. Boeuf and L. C. Pitchford, Phys. Rev. E **51**, 1376 (1995).